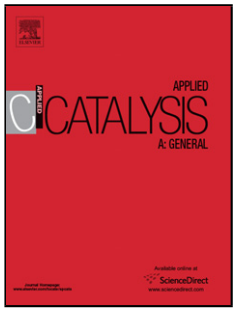

Title: Controlled manipulation of selectivity between O- versus C-alkylation in methylation of phenol using ZrO_2-WO_3-SiO_2

Authors: Kalpesh H. Bhadra, Ganapati D. Yadav

PII: S0926-860X(18)30254-0
DOI: https://doi.org/10.1016/j.apcata.2018.05.026
Reference: APCATA 16675

To appear in: *Applied Catalysis A: General*

Received date: 3-3-2018
Revised date: 8-5-2018
Accepted date: 23-5-2018

Please cite this article as: Bhadra KH, Yadav GD, Controlled manipulation of selectivity between O- versus C-alkylation in methylation of phenol using ZrO_2-WO_3-SiO_2, *Applied Catalysis A, General* (2018), https://doi.org/10.1016/j.apcata.2018.05.026

Revised Mns.: APCATA-D-18-00461
Sub: 8-May-2018

Controlled manipulation of selectivity between O- versus C-alkylation in methylation of phenol using ZrO_2-WO_3-SiO_2

Kalpesh H. Bhadra; Ganapati D. Yadav*

Department of Chemical Engineering

Institute of Chemical Technology

Nathalal Parekh Marg

Matunga

MUMBAI – 400 019

INDIA

***Author to whom correspondence should be addressed

Email: gdyadav@yahoo.com, gd.yadav@ictmumbai.edu.in

Telefax: +91-22-3361-1001, Fax: +91-22-3361-1002/1020

Graphical Abstract

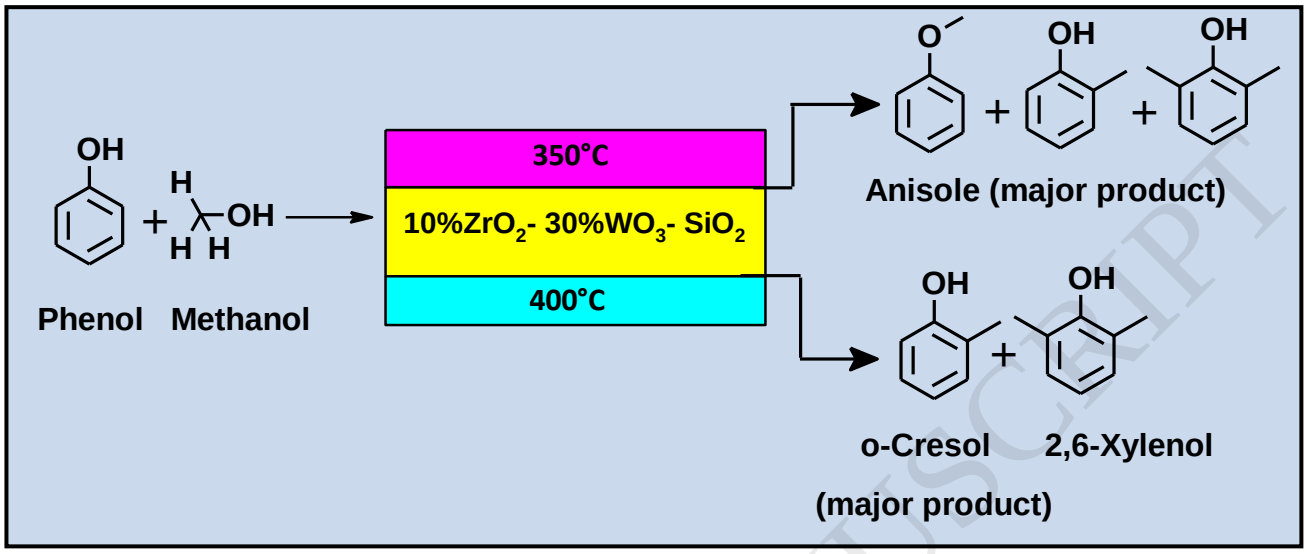

Highlights

- Synthesis of Zr, W and Si based mixed metal oxides for methylation of phenol.
- 10% ZrO_2- 30% WO_3-SiO_2 was the best for conversion of phenol and selectivity to anisole
- 10% ZrO_2- 30% WO_3-SiO_2 catalyst was stable up to 8 h
- Single catalyst for O and C-alkylation with manipulation of process conditions.

Abstract

Anisole and *o*-cresol are very important chemicals which could prepared from phenol using different catalytic routes favoring either O- or C-alkylation. In the methylation of phenol with methanol, the selectivity to either anisole or *o*-cresol could be manipulated using a suitable tailor-made catalyst having a proper balance of acidic and basic sites. In the current work, a series of compositions based on zirconium, tungsten and silicon oxides ($xZrO_2$-yWO_3-SiO_2) were prepared and employed as catalysts in fixed bed methylation of phenol. In the absence of silica as support, methylation of phenol over 20% WO_3-ZrO_2 and 40% WO_3-ZrO_2 favored predominantly C-alkylated product *o*-cresol. Among various combinations 10% ZrO_2-30% WO_3-SiO_2 gave the best

results and selectivity to the desired product anisole. Effect of various parameters affecting selectivity to anisole or *o*-cresol were studied systematically. The mechanism of formation of different products with reference to catalyst structure and functionality was explored in detail. The process parameters could be optimized to get the desired product. Thus, the proper choice can be made to choose the selectivity of *O*- versus *C*-alkylation using a single catalyst. The time on stream study was carried out for 16 h to find that the catalyst was stable and can be regenerated.

Keywords Alkylation; Phenol; Methanol; Anisole; Mixed metal oxide; Tungsten-zirconia based catalyst

1. Introduction

Phenol and phenolic derivatives have numerous applications in industries particularly for alkylated phenols. Methylation of phenol is extensively carried out to produce a variety of products such as as anisole, methylanisole, cresols and xylenols because of their industrial and commercial applications. In methylation of phenol, a number of O and C alkylated products are formed which are valuable in different applications; for instance, *o*-cresol is used as an intermediate in the synthesis of herbicides. 2,6 Xylenol is a monomer used for the synthesis of poly-(2,6-dimethyl)phenylene oxide resin. Trimethyl phenol is used as a starting material for the synthesis of vitamin E. Anisole and other methyl aryl ethers have applications as octane boosters for gasoline [1,2]. In conventional processes, alkylation of phenol to anisole is carried out using alkylating agents such as methyl iodide and dimethyl sulfate [3,4]. However, these processes are not environment friendly because alkali is used as a proton remover from phenol, the alkylating agents are toxic and pollution is caused due to large quantities of dissolved solids in the aqueous effluent, corrosion of equipment, etc. Extensive research has been carried out on alkylation of phenol using different alcohols and ethers using solid acid catalysts. For instance, tert-butylation of phenol and phenolic derivatives with tert-butanol and tert-butyl methyl ether [5,6], and isopropylation of phenols with isopropyl alcohol to synthesize propofol (2,6-diisopropyl phenol) which is general

anesthetic [7,8]. Alkylation using alkene such as cyclohexene and isobutylene has also been reported [9,10].

For methylation of substituted aromatics, methanol and dimethyl carbonate are used as alkylating agents. Alkylation of phenol with dimethyl carbonate using solid base catalyst selectively produces anisole but in batch process [11,12]. With methanol as an alkylating agent reactions are performed in vapor phase either with solid acids or solid base catalysts. Numerous researches have been reported on vapor phase methylation of phenol like alkali metal loaded silica [13], rare earth promoted metal phosphates [14], sulfates supported on gamma-alumina [15] and alkali loaded zeolites [16] which gave selective O-alkylated product whereas metal oxide catalysts such as MgO [17], Mg-Al-hydrotalcite [18], TiO_2 [19] , silica-manganese mixed oxide [20], V_2O_5-ZrO_2 [21], and spinel catalysts like $CoFe_2O_4$ [22], $Cu_xMn_{3-x}O_4$ [23], Mg/Fe/O [24] generated specifically C-alkylated products either *o*-cresol or 2,6-xylenol. Bronsted acid catalysts like Nafion-H resin, HY-zeolite, H-beta zeolites and heteropoly acid (HPA) on silica generated mixtures of anisole, *o*-cresol, xylenols and methyl anisole at lower temperatures [25-30]. In all of the above studies, it is seen that these catalysts either give O- or C-alkylated product or mixture of both. But there is no specific catalyst combination is available so far in literature as per our knowledge, which can generate both kinds of products in selective amount by modifying process parameters.

The foregoing literature survey shows that numerous catalyst systems have been reported for methylation of phenol. However, our objective was to design and develop a better catalyst which could be used at milder conditions as well as to make predominantly either anisole or cresol depending on the market and thus tuneability was very important. We initially targeted anisole as the product of choice since the reported catalysts have shown very poor selectivity to anisole. Anisole can be used to produce a number of products useful in fine chemical and pharmaceutical industries. ZrO_2-WO_3 as a binary mixed oxide has been used for organic reactions. Vapor phase methylation of phenol was planned in a fixed bed using a series of mixed oxides of Zr and W to understand product profiles and to study selectivity between C-alkylation leading to o-cresol or O-alkylation to anisole. Also there are no special reports are available on the use of ZrO_2-WO_3-SiO_2 containing mixed metal oxide catalyst for vapor phase methylation reaction which is the subject of current work. The manipulation of selectivity between anisole and 0-cresol using different conditions in the same catalyst was also targeted.

Thus, we are reporting the synthesis of a series of $xZrO_2$-yWO_3-SiO_2 catalysts and their application in vapor phase methylation of phenol. The present study involves optimization of best catalyst composition and process parameters such as WHSV (Weight hourly space velocity), mole ratio, temperature and stability of best catalyst in terms of time of stream study (TOS).

2. Experimental

2.1 Materials

Phenol (LR grade), methanol (HPLC grade), zirconium oxychloride (LR grade), 25% ammonia solution (all from S.D. fine chem., Mumbai, India), ammonium metatungstate (alfa aesar, Mumbai) and aerosil pharma-300 (fumed silica, Evonik Inc., Mumbai) were procured.

2.2 Catalyst synthesis and characterization

The mixed oxide catalysts of different compositions of ZrO_2 and WO_3 supported on fumed silica were prepared by impregnation technique. The total loadings of ZrO_2 and WO_3 were managed to 40% w/w on silica. In each sample of catalyst, however the corresponding loadings of ZrO_2 and WO_3 varied from 0 to 40%.

In typical synthesis of 10% ZrO_2- 30% WO_3- SiO_2, initially fumed silica (2.7 g) was dispersed in methanol. Required amount of zirconium oxychloride (1.18 g) was added drop wise in aqueous solution with continuous stirring. In the next stage, aqueous ammonia solution was added to the above solution till the pH of solution reached to 9. Mixing of the solution was continued for 2 h. Then water was evaporated with rotary evaporator and material was dried overnight at 110 °C. Aqueous solution of ammonium metatungstate (1.43 g in 20 ml D/I water) was added drop wise to the above dried material with continuous stirring for 3 h. Water was then evaporated and the resulting dried material was calcined in air at 750 °C for 3 h. Similarly, other combinations of variable percentages of ZrO_2 and WO_3 were loaded on silica. The series of catalysts prepared by the described procedure as above and denoted as *x*Zr-*y*W-SiO_2 where x and y represent the percentage of corresponding metal oxide denoted with initials as Zr and W respectively.

Powder X-ray diffraction pattern of all catalyst samples were recorded on X-ray diffractometer (Brucker) using Cu Kα using Cu Ka radiation (l = 1.540562). Infrared spectra were recorded on Perkin-Elmer instrument and in each case the sample was referenced against a blank KBr pellet. Surface area measurements and pore size distributions analysis were done by nitrogen adsorption on Micromeritics ASAP 2020 instrument at an adsorption temperature 77 K, after pre treating the sample under high vacuum at 250 ºC for 4 h. Scanning electron micrographs and elemental analysis was done by FEI, QUNTA 200 instrument. The ammonia- TPD data were recorded for all catalyst samples using AutoChem II 2920 TPD/TPR instrument (Micromeritics, USA) by using 10% NH_3 in He.

2.3 Reactor setup and procedure

The vapor phase reaction of phenol with methanol was carried out in vapor phase reactor of the dimensions ID 8 mm, OD 19 mm and length 400 mm (Chemito Technologies Pvt. Ltd., Nashik, India). Reactor was provided with temperature sensor (T1) at the bottom to read the temperature of reaction mixture during flow of reaction mass through the reactor. The reactor was equipped with HPLC pump (1) for constant volume flow of reaction mixture, pre-heater supplied to just before the reactor so that reaction mixture was vaporized before entering the reactor. MFC (mass flow controller) for continuous and constant flow of nitrogen gas was connected to the output from pre-heater (2) before entering the reactor. Nitrogen gas creates inert atmosphere also act as a carrier gas. Input from MFC, pre-heater and HPLC pump were connected to the reactor. The reactor was provided with furnace to heat it at higher temperature range up to 500 °C.Output from reactor was connected to condenser (provided with chiller) to condense the vapors of reaction mass and samples collected at time intervals from the condenser. Temperature of the entire system was maintained by digital temperature controller, and pressure of nitrogen gas was regulated by a regulator. The basic diagram of reactor set up is shown in Scheme 1.

3. Results and discussion

3.1 Catalyst characterization

3.1.1 X-ray diffraction (XRD)

The XRD patterns of all catalysts are shown in Figure 1. XRD pattern of 40% ZrO_2-Silica catalyst, shows no sharp peaks of zirconia phases are observed. However, with introduction of WO_3 species in next catalyst sample, 30% ZrO_2-10% WO_3-SiO_2, tetragonal phases of zirconia at 2θ values of 30° (111), 50° (220), and 60° (311) could be seen. Formation of tetragonal phases of ZrO_2, explains the role of WO_3 species in stabilizing the phases of zirconia [31-33]. However, WO_3 peaks started to be visible from 20% loading and above. Presence of peaks at 23-25° represent the monoclinic phase of WO_3 [34,35]. These intense peaks indicate the aggregation of WO_3 species leading to WO_3 microcrystallites on the surface of ZrO_2-SiO_2. The average crystallite size of all catalyst samples was calculated using Scherer equation. It was found that crystallite size increased with increase in WO_3 loading. The values of crystallite size are as follows. (a) 40% ZrO_2- SiO_2 (N.D.) (b) 30% ZrO_2-10% WO_3- SiO_2 (5.15 nm) (c) 20% ZrO_2- 20% WO_3-SiO_2 (41.21 nm) (d) 10% ZrO_2- 30% WO_3-SiO_2 (47.24 nm) (e) 40% WO_3- SiO_2 (32.31 nm). These structural changes are thought to make the catalysts more effective in performance with increased tungstate species.

3.1.2 FTIR spectroscopy

The FTIR results are shown in Fig.2a and 2b. No distinct peaks between Zr-O-Zr and W-O-W vibrations were observed because of high silica content. Broad range peaks in the range of 3200-3600 cm^{-1} represents the O-H stretching vibrations associated with silanol groups whereas the band near ~1630 cm^{-1} are O-H bending vibrations due to the physically adsorbed water on silica surface. The band at 1100-1200 cm^{-1} is due to siloxane bond (Si-O-Si). Apart from these peaks, two peaks at 752 and 710 cm^{-1} can be attributed to the W–O–W stretching vibration of monoclinic WO_3 (Fig. 2b) [36-38]. The weak band at 791 cm^{-1} is assigned to W-O vibration and this band possibly is due to both crystalline and non-crystalline species. This observation is supported by XRD pattern which showed the presence of monoclinic WO_3 crystallites [32]. The strong absorption peaks near 510 cm^{-1} correspond to the Zr–O vibrational modes [39, 40].

For further understanding, FTIR spectra of as such WO_3 and ZrO_2 were compared (Figure 2b). Here few observations could be made. In case of ZrO_2, a sharp band near ~800 cm^{-1} was observed which became weak when observed in 40% ZrO_2-SiO_2. Similarly, a broad band was observed in case of WO_3 in the range of 400-1000 cm^{-1}. This broad band became mild and sharp in case of

40% WO_3-SiO_2. The increase in band broadening near 800 cm^{-1} is due to increasing content of WO_3. This variation was observed in case of all ZrO_2-WO_3-SiO_2 combinations (Fig. 2a).

3.1.3 BET Surface area and pore analysis

The textural properties of catalysts by nitrogen adsorption-desorption measurements are given in Table 1. Fumed silica has a surface area of 306.1 m^2/g and pore volume of 0.774 cm^3/g and pore diameter of 10.1 nm. Comparison of nitrogen adsorption-desorption isotherm of silica and various catalysts are shown in Fig. (a-f) . The isotherms are of type IV with H1 hysteresis loop where initially nitrogen is adsorbed on catalyst surface slowly at low relative pressure which indicates the monolayer–multi layer adsorption on the surface. With increase in loading of zirconia and tungstate, the corresponding surface area of SiO_2 was found to decrease. Pore volume was decreased with marginal difference; however, important changes were found in pore sizes. Instead of decreasing, on loading ZrO_2 and WO_3 on silica, pore size increased. It may be because initially the surface and pores of silica are covered by zirconia and then loading of WO_3 takes place on the surface of ZrO_2-SiO_2 which increases the pore size of the catalyst. High intensity peaks (23-25°) in XRD (Fig. 1) represent crystalline phases of WO_3 supporting these changes on the surface of catalyst.

3.1.4 Acidity measurements

Acidity of catalyst samples was measured by temperature programmed desorption of ammonia (NH_3-TPD, Table 2). Two types of acidity were found in all catalyst samples. Weak acidity peaks were observed in the range of 120-140 °C. The strong acidity peaks were observed around 670-750 °C. These peaks indicate both type of acidic properties are present in catalysts. Increased WO_3 content increases the acidity. 40% WO_3-SiO_2 showed highest acidity value of 0.687 mmol/g of ammonia (combining weak and strong acidity values). Figure 4 shows the acidity pattern of catalysts.

3.1.5 SEM/EDXS analysis

SEM images of catalysts are shown in Figure 5. There are no marked differences in images of all catalyst samples. Elemental composition of catalysts was confirmed by EDXS method. Typical EDXS elemental composition for 10% ZrO_2- 30% WO_3-SiO_2 shown in Figure 6. Table 3 represents the compositions of $x$$ZrO_2$-$y$$WO_3$-$SiO_2$ series catalysts. Since the silica used in the catalyst preparation is fumed silica, irregular shape and sizes of particles are observed in the images and the particle size also varied from 10 µm to 60 µm.

3.2 Catalyst activity

3.2.1 Material balance and product distribution

For material balance, reaction pathways shown in Scheme 2 were considered. But under all experimental conditions used in this work, 2-methyl anisole (E) and 2, 4, 6-trimethyl phenol (F) were not formed. Pathway 1 leads to anisole (B) which does not lead to 2-methyl anisole subsequently. Pathway 2 goes to o-cresol (C) and subsequently 2,6- xylenols (D). Rearrangement of anisole (B) to *o*-cresol (C) is one of the possible the reactions. It was observed that during the course of reaction, selectivity of anisole decreased and that of *o*-cresol increased. It can be said that the rearrangement reaction is one of most probable pathway for the formation of *o*-cresol apart from direct C-alkylation of phenol. Since methanol was used in excess in all the sets of experimental conditions, dimethyl ether was also formed due to dehydration of methanol, formation of which is not shown in Scheme 2. Carbon balance was also done to find that formation of products could be accounted for all organic compounds and ~10-12% carbon was deposited after 6 h.

In order to understand the reaction mechanism and further improvement in the process to get desired products like anisole and *o*-cresol following three sets of experiment were planned.

1. Reaction of phenol and methanol
2. Rearrangement of anisole to *o*-cresol to confirm rearrangement reaction
3. Methylation of *o*-cresol to 2,6- xylenol. *3.2.2 Efficacy of catalysts*

Independent experiments were also done to understand reaction mechanism and product profile under identical conditions. As given before three sets of experiments were performed: (i) reaction

of phenol and methanol, (ii) rearrangement of anisole to o-cresol to confirm rearrangement reaction, and (iii) methylation of o-cresol to 2,6- xylenol. In particular, 20%WO_3-ZrO_2 and 40% WO_3-ZrO_2 were prepared as per procedure mentioned in Section 2.2 without using fumed silica. These two catalysts were also tested under the same reaction conditions. In case of 20%WO_3-ZrO_2, conversion of phenol after 6 h was 45% with anisole selectivity of 25% whereas *o*-cresol selectivity was found to 53.7% (Figure (7a, 7b). Increasing amount of WO_3, 40% WO_3-ZrO_2 led to 51.4 % conversion of phenol with selectivity of anisole and *o*-cresol found to be 38.4 % and 47.2%, respectively (Fig. 8a,8b). However, major drawback of these two catalysts was formation of 2,6-xylenol, trimethyl phenol (TMP) and other alkylated derivatives of phenol. 2,6-Xylenol formation was found 11.2% and 10.2% in 20% WO_3-ZrO_2 and 40% WO_3-ZrO_2 respectively. Whereas other impurities and TMP together constituted 9.9% and 4.3% in the case of 20%WO_3-ZrO_2 and 40% WO_3-ZrO_2, respectively. Then we thought of using SiO_2 as a support and tested in the reaction where anisole selectivity was improved as compared to the above catalysts. So, a series of $xZrO_2$-yWO_3-SiO_2 catalysts were prepared to tune the selectivity. Here the role of silica in the ternary oxide system can be understood. Silica dilutes the activity of other two oxides and limits the formation of impurities as well as increases the selectivity of anisole and o-cresol based on variable compositions of other two oxides.

Initially a series of catalysts $xZrO_2$ - yWO_3 - SiO_2 were tested to evaluate their activity and selectivity in vapor phase methylation of phenol. For screening of catalysts, typical reaction conditions were as follows. Phenol : methanol mole ratio-1:5, catalyst quantity - 2 g, temperature - 623 K, WHSV- 1 h^{-1} and nitrogen gas flow- 30 ml/min. Reaction was continued for 6 h. Conversion of phenol and anisole selectivity profiles are depicted in Figure 9(a) and (b). In results, it was found that steady state condition was achieved only after 4^{th} h in all catalyst combinations; however, selectivity of anisole was found to decrease in all the combinations of catalysts except 20% ZrO_2-20%WO_3-SiO_2, where conversion of phenol and selectivity of anisole remained constant after the steady state (i.e. 3 h). In the case of 10% ZrO_2 - 30% WO_3 - SiO_2, steady state condition was achieved after 4 h with 47 % conversion of phenol and 52 % anisole selectivity; hence 10% ZrO_2 - 30% WO_3 - SiO_2 was selected for further reaction parameters optimization. It was observed that increasing amount of WO_3 in catalyst increases the conversion of phenol as well as improves the selectivity towards anisole but 40% WO_3 -SiO_2 gave lesser conversion because of

presence of monoclinic WO_3 phase. Monoclinic WO_3 at 2θ=23- 25° is known as boundary point of decreasing activity [37]. The experimental results thus prove that only ZrO_2 or only WO_3 supported on silica may not give good results but the combination of both the oxides can give better conversion and selective formation of anisole. The tetragonal phase of ZrO_2 is stabilized by addition of WO_3 (as revealed by XRD characterization) which further improved acidity of the catalyst combinations (as found by ammonia TPD results). These two factors probably improved activity of catalysts in terms of conversion of phenol and selectivity of anisole in a ternary mixture of $xZrO_2$-yWO_3-SiO_2.

To understand the mechanism by which there is a decrease in anisole selectivity during the course of reaction, two more sets of experiment were conducted.

Set-1 experiment included methylation of *o*-cresol at different temperatures with optimized catalyst 10% ZrO_2 - 30% WO_3 - SiO_2 by maintaining *o*-cresol: methanol mole ratio as 1:5 and WHSV as 1 h^{-1}, catalyst weight – 2 g and N_2 gas flow maintained at 30 ml/min (Fig. 10a). The purpose of this set of experiment was to confirm the pathway of methylation of phenol. In the case of *o*-cresol, *o*-methyl anisole (*o*-MAN) formed as highly selective product at 573K (72 %) and 623K (~64%) and its selectivity remained nearly the same throughout the course of reaction (Figure 10a). However, rearrangement of *o*-methyl anisole (*o*-MAN) to 2,6-xylenol was observed at 673 K with constant conversion of o-cresol (~34%) (Figure 10b). These results are in agreement with the one obtained during methylation of phenol done by us.

Set-2 experiment included only anisole to be passed through the catalyst bed of 2 g 10% ZrO_2-30% WO_3- SiO_2 at different temperatures, while other reaction parameters were the same as above. The product profile in this reaction is somewhat complex to understand. At low temperature 573 K, anisole conversion found very low (~10% after 6 h of reaction), with higher selectivity for *o*-methyl anisole (*o*-MAN, ~75% at 6^{th} h) and phenol as another product (25% at 6^{th} h) (Figure 11a and 11b). The formation of *o*-MAN and phenol is possible through the first reaction given below in Scheme 3. At 623 K, phenol formation is almost constant (~45%) whereas *o*-MAN selectivity was found decreasing (from 50% to ~20% at the end of 6 h) with gain in selectivity of *o*-cresol (from ~7 % to 23 % at the end of 6 h) and 2,6-xylenol (from 0 % to ~12 % at the end of 6 h) (Figure 9b). Conversion of anisole was found to be ~57 % after 6 h. At 673 K, 94 % of anisole

was converted and hence more side products were observed like other isomers of xylenol, 2,4,6-trimethyl phenol and duranol (Figure 11c). The increased formation of *o*-cresol is a result of reactions 2 and 4 given in Scheme 3. Phenol is the product in most of the steps (1, 2 and 3) whereas *o*-MAN is formed initially and then involved in formation of *o*-cresol. These observations prove that there is a rearrangement of aryl ethers to respective phenolic compound and rest of the products formed are because of following set of reactions given in Scheme 3. The results are comparable to the one obtained by Prasomsri et al [38].

From the above sets of experiments, it can be concluded that O-methylation of phenolic molecules is a first step of reaction and then there is a rearrangement of anisole to *o*-cresol (in case of methylation of phenol) and *o*-MAN to 2,6- xylenol (in case of methylation of *o*-cresol).

3.3 Optimization of process parameters

3.3.1 Effect of WHSV

Effects of WHSV were studied in the range from 1 to 3 h^{-1}, maintaining mol ratio, phenol : methanol (1:5), catalyst weight (10% ZrO_2 - 30% WO_3 - SiO_2) – 2g and temperature maintained at 623 K in presence of nitrogen flow rate- 30 ml/min. With increase in WHSV from 1 to 3 h^{-1}, conversion of phenol decreased (Figure 12). The probable reason for decreasing conversion is the lesser contact time. However, the selectivity of anisole increased with increased WHSV. Because of lesser contact time, the rearrangement of anisole to *o*-cresol is inhibited. In comparison, WHSV of 1 h^{-1} gave higher conversion of phenol (47%) as well as good anisole selectivity (52%) at 6^{th} h; hence further reactions were carried out with WHSV of 1 h^{-1}.

3.3.2 Effect of mole ratio

Mole ratio studies were carried out in range from 1:3 to 1:9 (phenol: methanol) over optimized catalyst, 10% ZrO_2- 30% WO_3-SiO_2 (2g) and optimized WHSV of 1 h^{-1}. The temperature of reaction was set to 623 K. The results are shown in Figure 13 (a) and (b). With increase in molar ratio from 1:5 to 1:9, the conversion of phenol was found to decrease because lower molar concentration of phenol (hence lower partial pressure of phenol) passed through the catalyst bed during the reaction and hence conversion was found to decrease [39]. However, anisole selectivity

was lowered in case of increasing mole ratio from 1:5 to 1:7 and 1:9. This inversion in selectivity of anisole may be due to increased concentration of methanol which provides more methyl groups to attack on reactive ortho positions of phenol ring resulting in formation of *o*-cresol and 2,6-xylenol. With this conclusion, in case of 1:3 mol ratio, the conversion was expected to increase but it did not show any such increment (Figure 13a). The probable reason for lower conversion (5.2%) may be due to excess molar concentration of phenol in reaction mixture lead to more coke formation and hence conversion was consistently decreased due to blockage of the active sites. Hence, mole ratio 1:5 was optimized for further study of temperature effects.

3.3.3 Effect of temperature

Temperature plays a crucial role in deciding conversion and selectivity of products in either liquid phase or vapor phase reaction. In temperature studies, reactions were carried out at temperature between 573- 673 K, maintaining the optimized reaction conditions of mole ratio of 1:5 and WHSV of 1 h^{-1} in each study. It was observed from the results (Figure 14a) that increased temperature (673 K) leads to lower conversion of phenol. The experiments were repeated and it was found that there was reduction in porosity due to carbon deposition on the catalyst surface. Because formation of o-cresol and xylenols followed by carbonization the selectivity to anisole decreased at 673 K. So the regenerated catalyst was found to give the same conversion and selectivity for 1 h and thereafter the same trend was observed as regards more byproducts and carbon formation.

At lower temperature of 573 K, conversion was less. Conversion and selectivity profile at various temperatures are shown in Fig 14 (a) and (b).

3.3.4 Time on stream (TOS) study

To understand the activity and stability of catalyst, time on stream (TOS) studies were conducted at optimized conditions of mole ratio of 1:5 (phenol: methanol), catalyst weight (2 g), WHSV (1 h^{-1}) and temperature (623 K) and nitrogen gas flow 30 ml/min. The reaction was continued for 16 h to check the stability of catalyst. Conversion of phenol was marginally decreased with time; however, from 10^{th} h onwards conversion started to decrease and reached to the final conversion of 38 % (Figure 15a); similar trend was observed in selectivity of anisole (Figure 15b). It was decreased linearly up to first 5 h and then remains stable up to 8 h. It means catalyst has stability

up to 8 h and hence it has to be regenerated to get consistent selectivity of anisole. From 8 h onwards, *o*-cresol increases until 16 h and remain constant. The decrease in conversion may probably due to the formation of coke on the surface of catalyst. The presence of carbon was confirmed and quantified from EDXS analysis. The total carbon content was found to be ~12%. Fig. 16 depicts the comparison of SEM image of fresh and spent catalyst after continuing reaction for 16 h. As per SEM images, the smooth surfaces of fresh catalyst are observed as rough in case of spent catalyst. The change in surface morphology is because of coke formation on the surface of catalyst. The elemental composition of fresh and spent catalyst showed differences as shown in Table 4. The carbon content in the spent catalyst was found up to ~12%. This generation of carbon on the surface of catalyst reduces the activity of catalyst after 16 h. Spent catalyst was also characterized by XRD and ammonia-TPD techniques to compare with the fresh catalyst as shown in Fig. 17 and 18, respectively. XRD comparison showed less intensity peaks in spent catalyst which supports the formation of coke on the surface of catalyst. However, there were no phase changes when compared with the fresh catalyst (Table 5). Ammonia –TPD thermograms of fresh and spent catalyst are given Fig. 18. The decrease in acidity of catalyst is due to coke formation on the surface of catalyst.

4. Conclusion

Methylation of phenol to anisole or o-cresol is industrially important. Vapor phase methylation was carried out successfully with a series of novel mixed metal oxide catalysts $x ZrO_2$-$y WO_3$-SiO_2. Amongst the series of catalysts, 10% ZrO_2-30% WO_3-SiO_2 was proved to be the best catalyst in terms of conversion and selectivity towards anisole. At 623K, anisole was found as a major product but on increasing temperature up to 673K, *o*-cresol selectivity increased. Increasing mole ratio leads to increased cresol selectivity. So, the reaction parameters were optimized by carrying out detailed studies. For anisole formation, optimized conditions are (1:5 Phenol: methanol mol ratio), WHSV- 1 h^{-1} and 623 K for 8 h. The great advantage of the catalyst is the switching of selectivity for desired product by manipulating reaction parameters. The catalyst 10% ZrO_2- 30% WO_3- SiO_2 was also found stable up to 8 h. Thus, methylation of phenol using 10% ZrO_2- 30% WO_3- SiO_2 is environmentally viable and benign process and it opens up the freedom of manipulating the

selectivity to either anisole or *o*-cresol using a single catalyst through choice of proper reaction parameters.

Conflict of Interest Statement

The authors declare no conflict of interest.

Acknowledgements

K.H.B. thanks UGC for providing JRF under its BSR programme in Green Technology.

G.D.Y. received support from R.T. Mody Distinguished Professor Endowment and J.C. Bose National Fellow of Department of Science and Technology, Government of India.

References

[1] J. E. Bailey, Bohnet M, Brinker J (eds) (1988) Ullman's encyclopedia of industrial chemistry, 6th edn. Willey-VCH,Weinheim.

[2] J. Kirk, K. Othmer, Encyclopedia of Chemical Technology, 3rd ed., Wiley–Inter science, New York, 1981.

[3] H. F. Lewis, S. Shaffer, W. Trieschmann, H. Cogan, Ind. Eng. Chem. 22 (1930)34–36.

[4] N. J. Hales, H. Heaney, J. H. Hollinshead, S. V. Ley, Tetrahedron 51 (1995) 7741–7754.

[5] G. D. Yadav, N. S. Doshi, Appl. Catal. A: Gen. 236 (2002) 129-147.

[6] S. E. Dapurkar, P. Selvam, J. Catal. 224 (2004) 178–186.

[7] R. Savidha, A. Pandurangan, Appl. Catal. A: Gen. 262 (2004) 1–11.

[8] K. Y. Nandiwale, V. V. Bokade, RSC Adv. 4 (2014) 32467-32474.

[9] G. D. Yadav, P. Kumar, Appl. Catal. A: Gen. 286 (2005) 61-70.

[10] K. Gokul Chandra, M. M. Sharma, Catal. Lett. 19 (1993) 309.

[11] Y. Ono, Appl. Catal. A: Gen.155 (1997) 133–166.

[12] S. T. Gadge, A. Mishra, A. Gajengi, N. V.Shahi, B. M. Bhanage, RSC Adv. 4 (2014) 50271-50276.

[13] R. Bala, S. Sivasanker, Appl. Catal. A: Gen. 246 (2003) 373–382.

[14] G. Sarala Devi, D. Giridhar, B. M. Reddy, J. Mol. Catal A: Chem. 181 (2002) 173–178.

[15] M. C. Samolada, E. grigoriadou, Z. Kiparissides, I. A. Vasalos, J. Catal. 152 (1995) 52-62.

[16] S. Chul Lee, S. Woo Lee, K. Seok Kim, T. Jin Lee, D. Hyun Kim, J. Chang Kim, Catal. Today. 44 (1998) 253-258.

[17] F. Cavani, L. Maselli, S. Passeri, J. A. Lercher, J. Catal. 269 (2010) 340–350.

[18] S. Velu, C.S. Swamy, Appl. Catal. A: Gen. 119 (1994) 241-252.

[19] A. R. Gandhe, J. B. Fernandes, S.Varma, N.M. Gupta, J. Mol. Catal. A: Chem. 238 (2005) 63–71.

[20] Y. Wang, Y. Song, W. Huob, M. Jia, X. Jing, P. Yang, Z. Yang, G. Liu, W. Zhang, Chem. Engg. J. 181 (2012) 630– 635.

[21] Komandur V. R. Chary, K. Ramesh, G. Vidyasagar, V. Venkat Rao, J. of Mol. Catal A: Chem. 198(2003) 195–204.

[22] N. Ballarini, F. Cavani, S. Passeri, L. Pesaresi, A. F. Lee, K. Wilson, Appl. Catal. A: Gen. 366 (2009) 184–192.

[23] A. S. Reddy, C. S. Gopinath, S.Chilukuri, J. Catal. 243 (2006) 278–291.

[24] V. Crocell`a,G. Cerrato,G. Magnacca, C. Morterra,F. Cavani,L. Maselliand S. Passeri, Dalton Trans. 39 (2010) 8527–8537.

[25] E. Santacesaria, D. Grasso, D. Gelosa, S. Carrá, Appl. Catal. 64 (1990) 83-99.

[26] S. Balsama, P. Beltrame, P.L. Beltrame, P. Carniti, Appl. Catal. 13 (1) (1984) 161-170.

[27] M. Bregolato, V. Bolis, C. Busco, P. Ugliengo, S. Bordiga, J. Catal. 245 (2007) 285–300.

[28] M. Marczewski, J-P. Bodibo, G. Perot, M. Guisnet, J. Mol. Catal. 50 (2) (1989) 211-218.

[29] M. E. Sad, C. L. Padró, C. R. Apesteguía, Appl. Catal. A:Gen. 475 (2014) 305-313.

[30] M. E. Sad, C. L. Padró, C. R. Apesteguía, Catal. Today. 133–135 (2008) 720-728.

[31] M. Scheithauer, R. Grasselli, K. Knozinger, Langmuir. 14 (1998) 3019- 3028.

[32] R. A. Boyse, E. I. Ko, J. Catal. 171 (1997) 191-207.

[33] D. Gazzoli, D, M. Valigi, R. Dragone, A. Marucci, G. Mattei, J. Phys. Chem. B. 168 (1997) 431-441.

[34] A. Martı´nez, G. Prieto, M. A. Arribas, P. Concepcio´n, J. F. Sa´nchez – Royo, J. Catal. 248 (2007) 288-302

[35] A. Martı´nez, G. Prieto, M. A. Arribas and P. Concepcio´n, Appl. Catal., A 309 (2006), 224-236.

[36] H. R. Sahu and G. R. Rao, Bull. Mater. Sci. 23 (2000) 349–354.

[37] E. I. Ross-Medgaarden, W. V. Knowles, T. Kim, M. S. Wong, J. Catal., 256 (2008) 108-125.

[38] T. Prasomsri, A. T. To, S. Crossley, W. E. Alvarez, D. E. Resasco, Appl. Catal. B. 106 (2011) 204-211.

[39] V. V. Bokade, G. D. Yadav, J. Mol. Catal. A: Chem. 285 (2008) 155–161.

[40] M. Marczewski, J. P. Bodibo, G. Perot, M.Guisnet, J. Mol. Catal. 50 (1989) 211-218.

[41] P. L. Beltrame, P. Carniti, A. Castelli, L. Forni, Appl. Catal. 29 (1987) 327-334.

[42] M. E. Sad, C. L. Padro´, C. R. Apesteguı´a, J. Mol. Catal. A: Chem. 327 (2010) 63-72.

[43] J. Kaspi, G. A. Olah, J. Org. Chem. 43 (1978) 3142-3147.

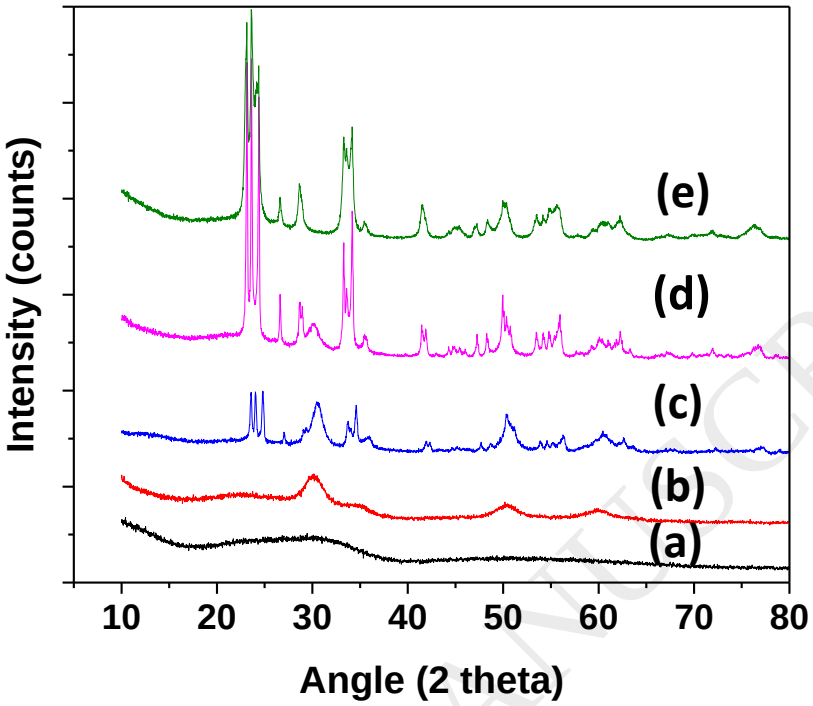

Figure1. XRD of *x*ZrO_2- *y*WO_3-SiO_2 series catalysts (a) 40% ZrO_2- SiO_2, (b) 30% ZrO_2 -10% WO_3- SiO_2, (c) 20% ZrO_2-20% WO_3- SiO_2, (d) 10% ZrO_2-30% WO_3- SiO_2 and (e) 40% WO_3-SiO_2

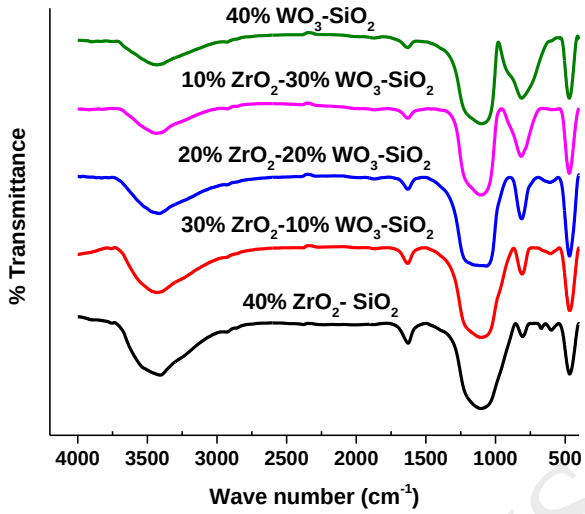

Figure 2(a). FTIR comparison of xZrO$_2$-yWO$_3$-SiO$_2$ series catalysts

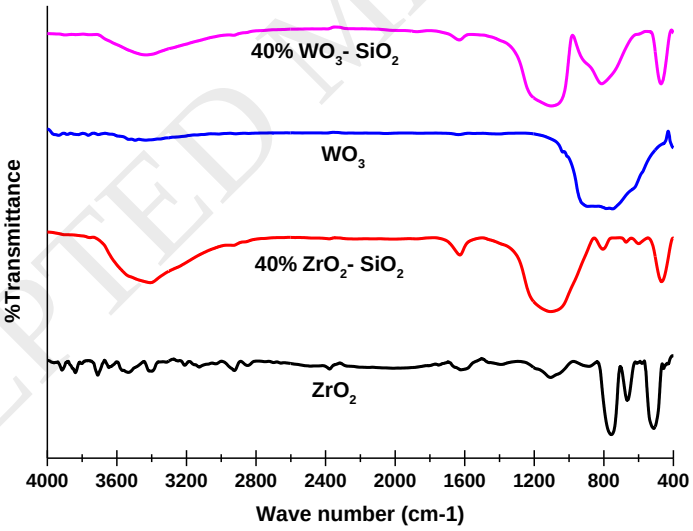

Figure 2(b). FTIR comparison of ZrO$_2$ and WO$_3$ with 40% ZrO$_2$-SiO$_2$ and 40% WO$_3$- SiO$_2$

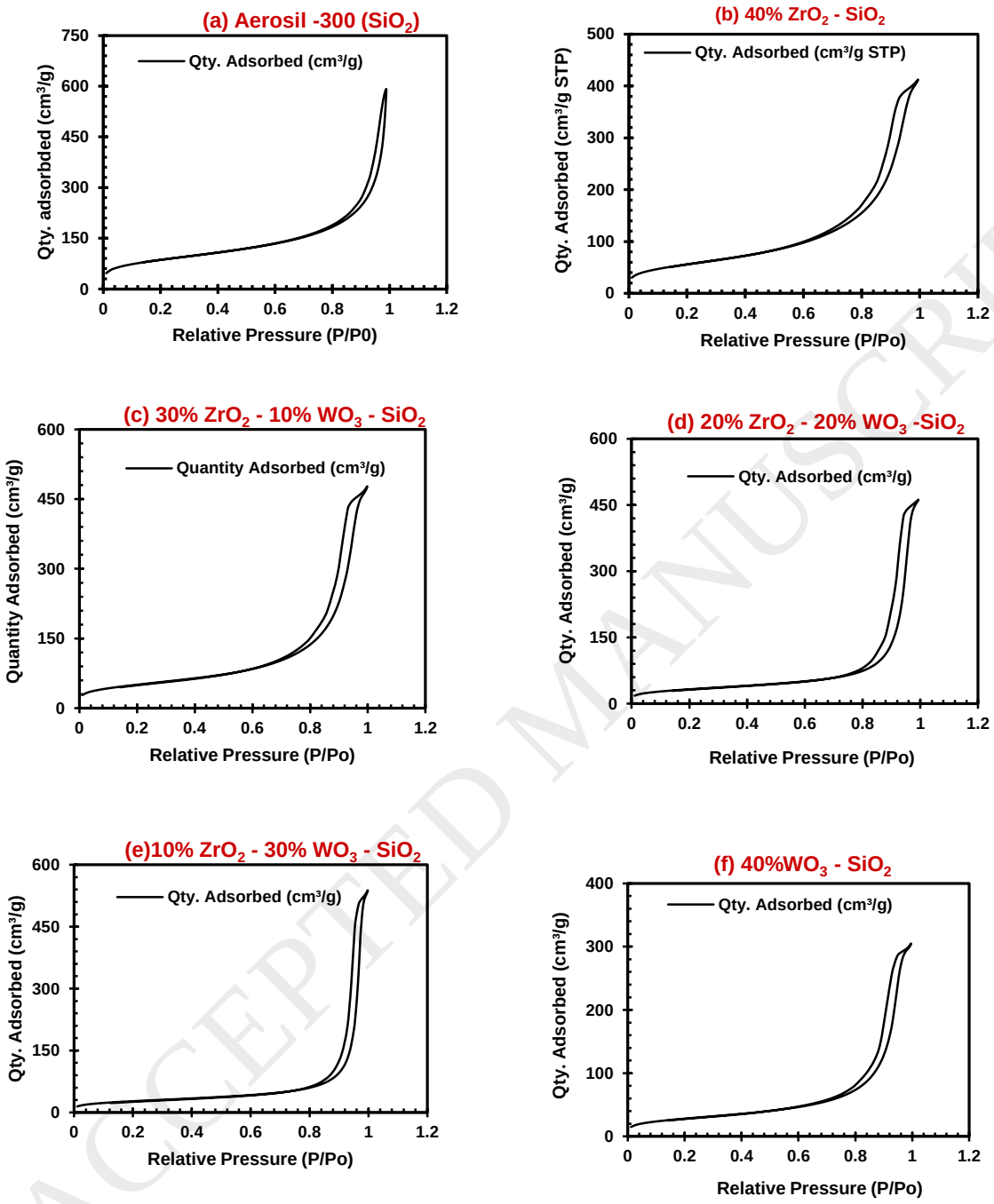

Figure 3. N_2 adsorption-desorption isotherms of $x ZrO_2$-$y WO_3$-SiO_2 series catalysts at 77 K

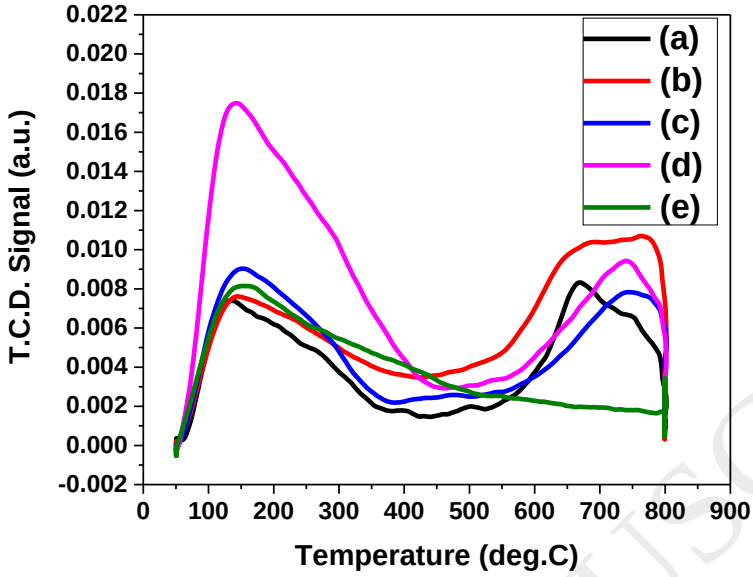

Figure 4. Ammonia-TPD thermograms of xZrO$_2$-yWO$_3$-SiO$_2$ series of catalysts. (a) 40% ZrO$_2$-SiO$_2$, (b) 30% ZrO$_2$-10% WO$_3$- SiO$_2$, (c) 20% ZrO$_2$- 20% WO$_3$- SiO$_2$, (d) 10% ZrO$_2$- 30% WO$_3$-SiO$_2$ and (e) 40% WO$_3$- SiO$_2$

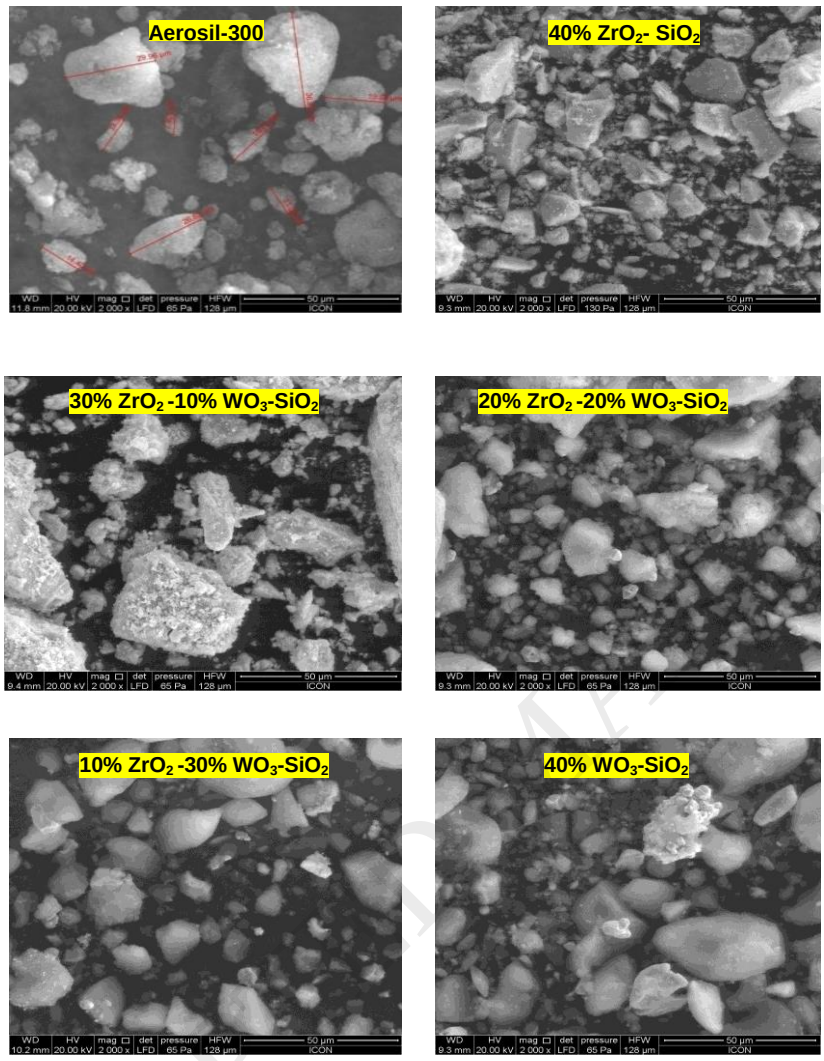

Figure 5. SEM images of fumed silica and $xZrO_2$- yWO_3 - SiO_2 series catalysts at magnification 2000x

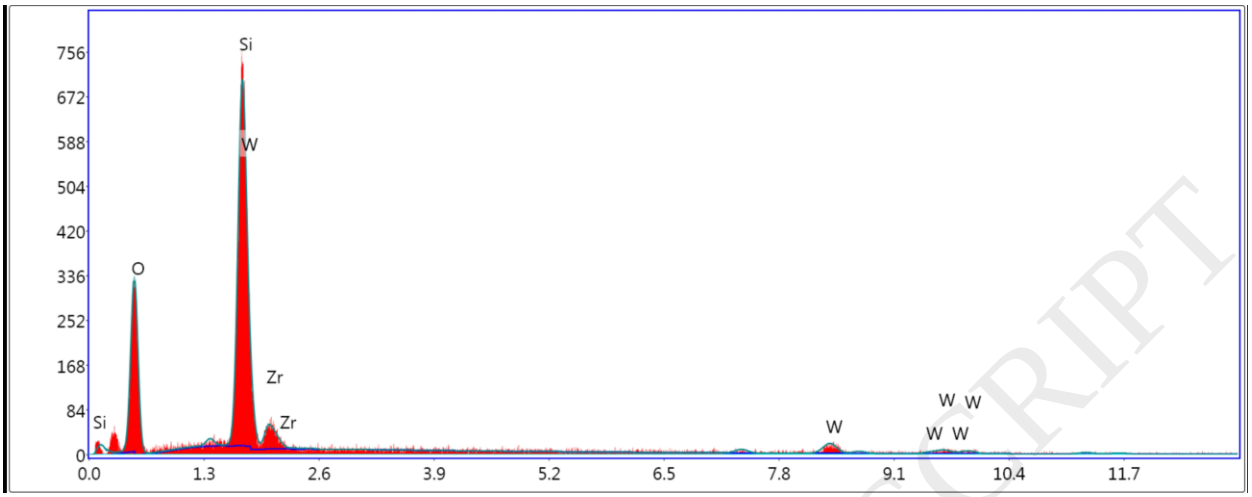

Figure 6. EDXS analysis of xZrO$_2$- yWO$_3$ - SiO$_2$ series catalysts

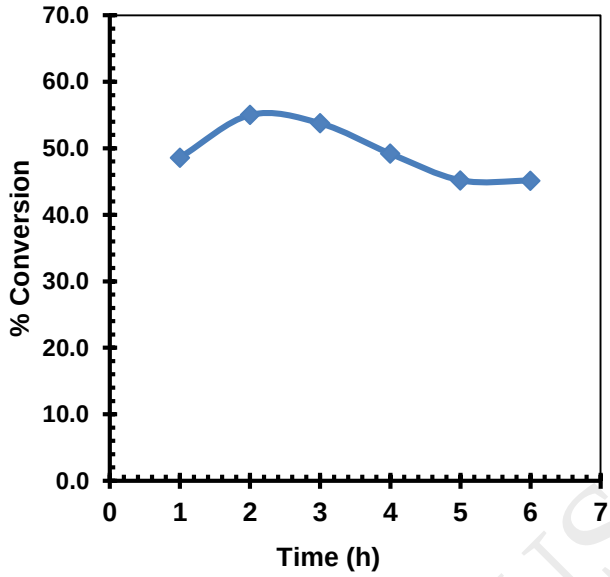

Figure 7(a). Phenol conversion profile with 20% WO_3-ZrO_2 catalyst. Reaction conditions - Phenol: methanol (1:5) mole, catalyst – 2 g, WHSV – 1 h^{-1}, temperature – 623 K, N_2 flow – 30 mL/min

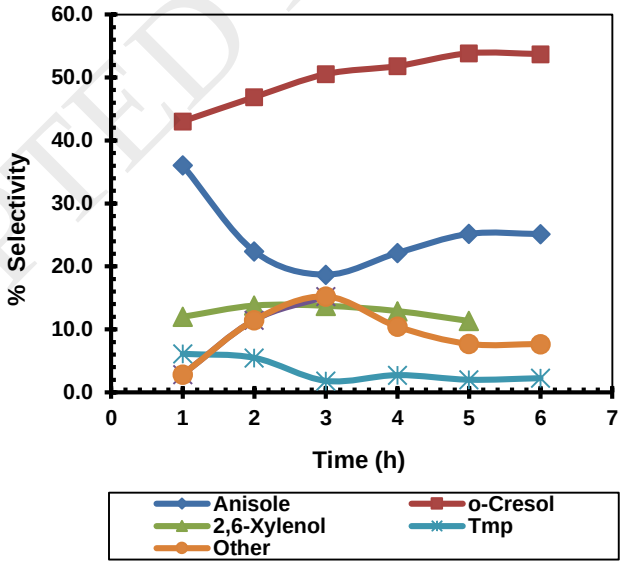

Figure 7(b). Selectivity profile with 20% WO_3-ZrO_2 catalyst. Reaction conditions - Phenol: methanol (1:5) mole, catalyst – 2 g, WHSV – 1 h^{-1}, temperature – 623 K, N_2 flow – 30 mL/min

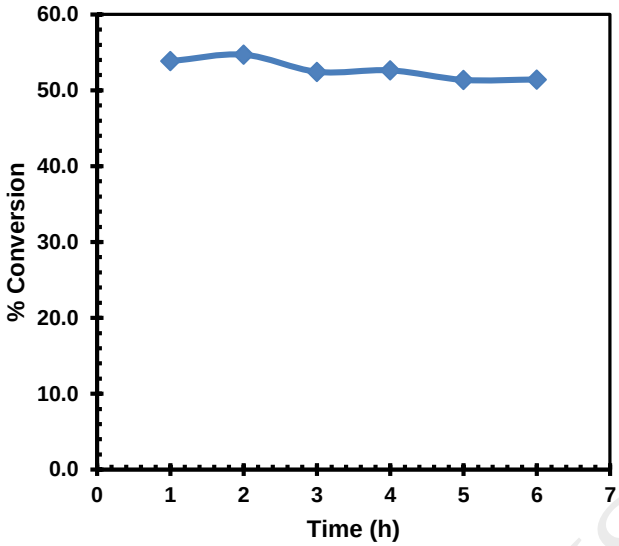

Figure 8(a). Phenol conversion profile with 40%WO_3-ZrO_2 catalyst. Reaction conditions - Phenol: methanol (1:5) mole, catalyst – 2 g, WHSV – 1 h^{-1}, temperature – 623 K, N_2 flow – 30 mL/min

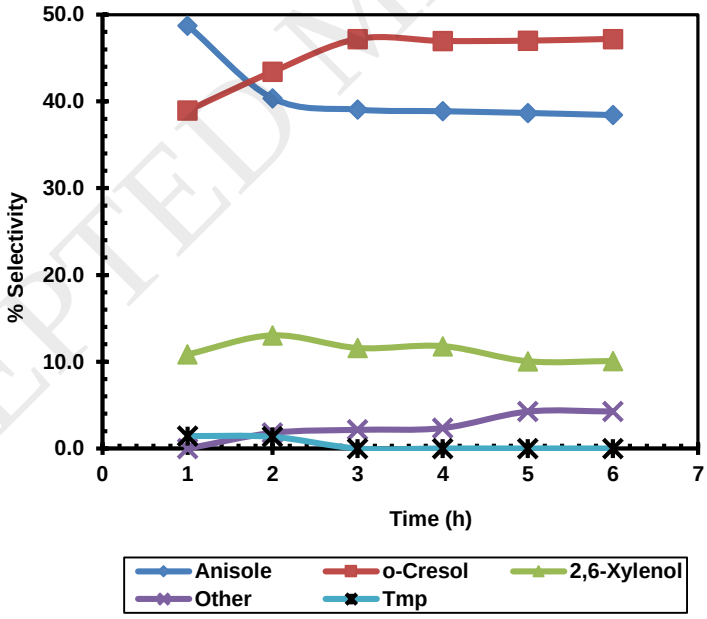

Figure 8(b). Selectivity profile with 40%WO_3-ZrO_2 catalyst. Reaction conditions - Phenol: methanol (1:5) mole, catalyst – 2 g, WHSV – 1 h^{-1}, temperature – 623 K, N_2 flow – 30 mL/min

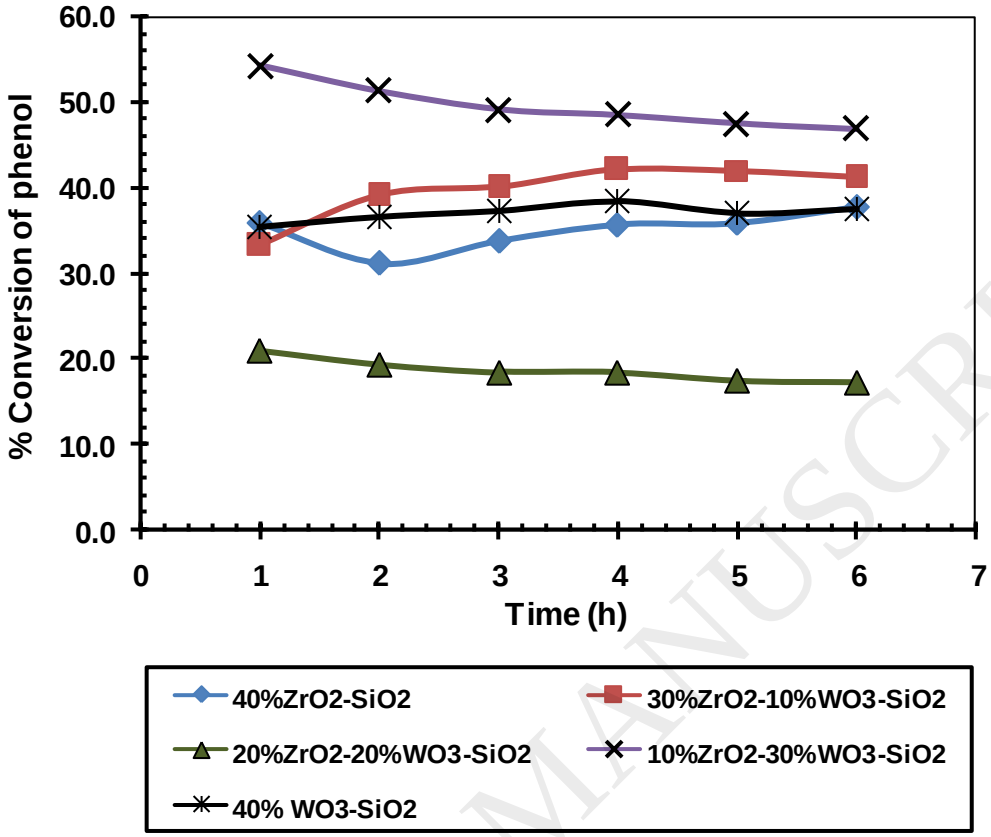

Figure 9(a). Phenol conversion profile with different catalysts. Reaction conditions - Phenol: methanol (1:5) mole, catalyst – 2 g, WHSV – 1 h^{-1}, temperature – 623 K, N_2 flow – 30 mL/min, time – 6 h

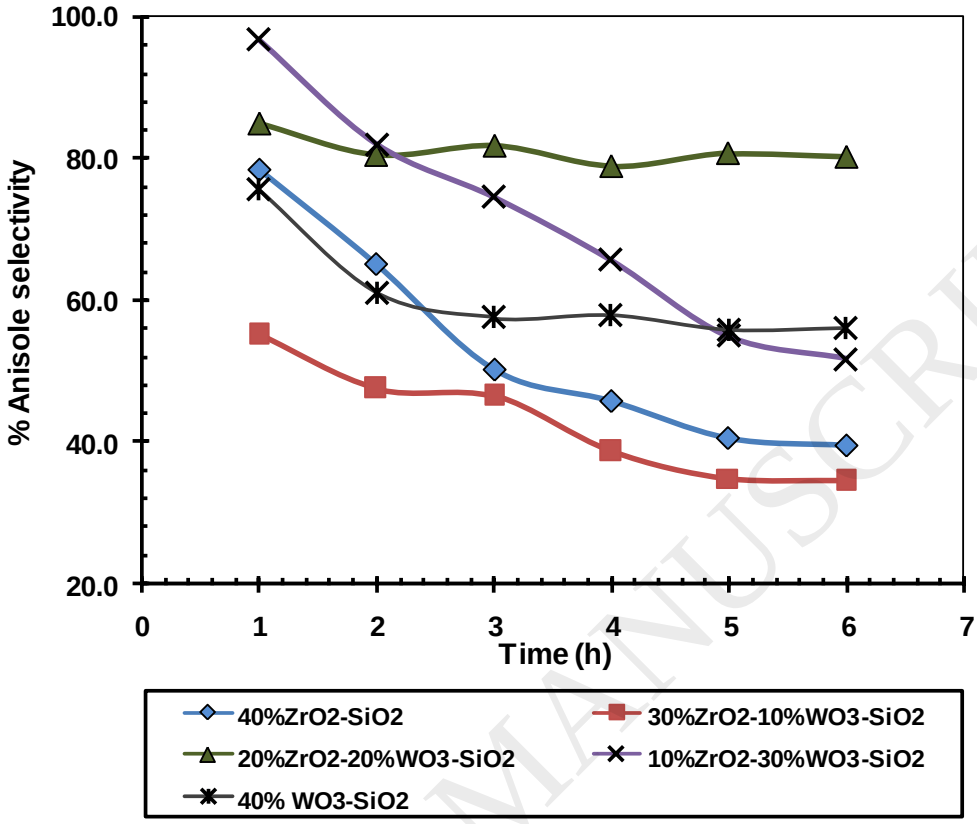

Figure 9(b). Anisole selectivity profile with different catalysts. Reaction conditions- Phenol: methanol (1:5) mole, catalyst – 2 g, WHSV – 1 h^{-1}, temperature – 623 K, N_2 flow – 30 mL/min, time – 6 h

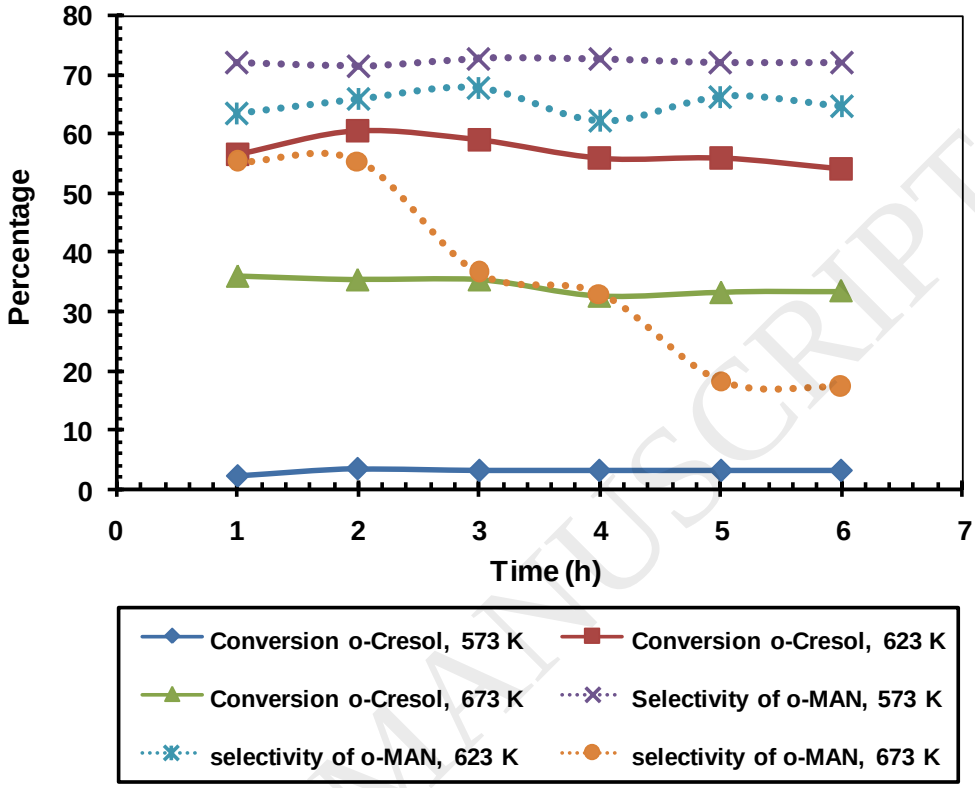

Figure 10(a). *o*-Cresol conversion and *o*-methyl anisole selectivity during methylation of *o*-cresol with 10%ZrO_2-30%WO_3-SiO_2 at different temperatures. Reaction conditions- *o*-Cresol: methanol (1:5) moles, catalyst – 2 g, WHSV – 1 h-1, N_2 flow – 30 mL/min

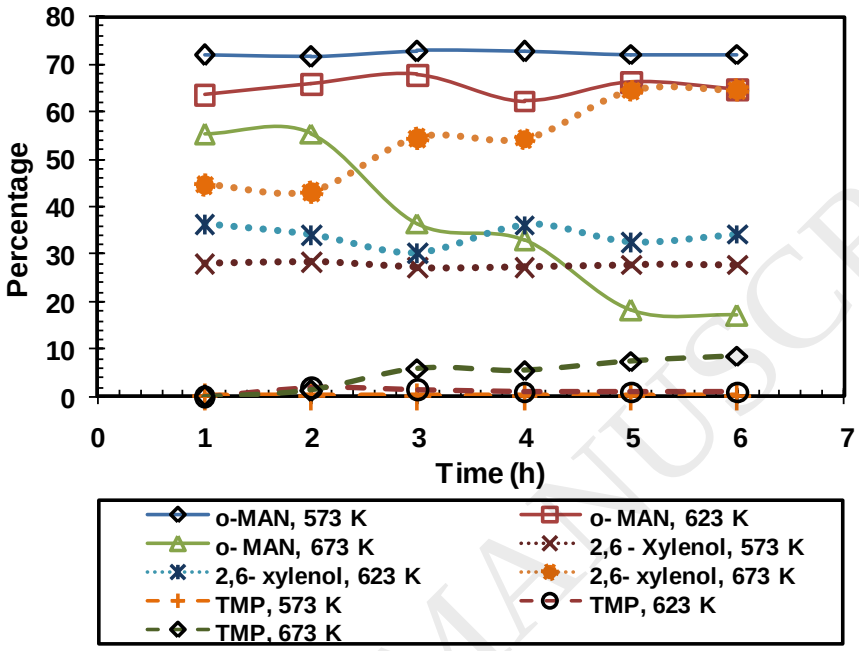

Figure 10(b). Products profile of methylation of *o*-Cresol at different temperatures. Reaction conditions- *o*-Cresol: methanol (1:5) mole, catalyst – 2 g, WHSV – 1 h^{-1}, N_2 gas flow – 30 mL/min

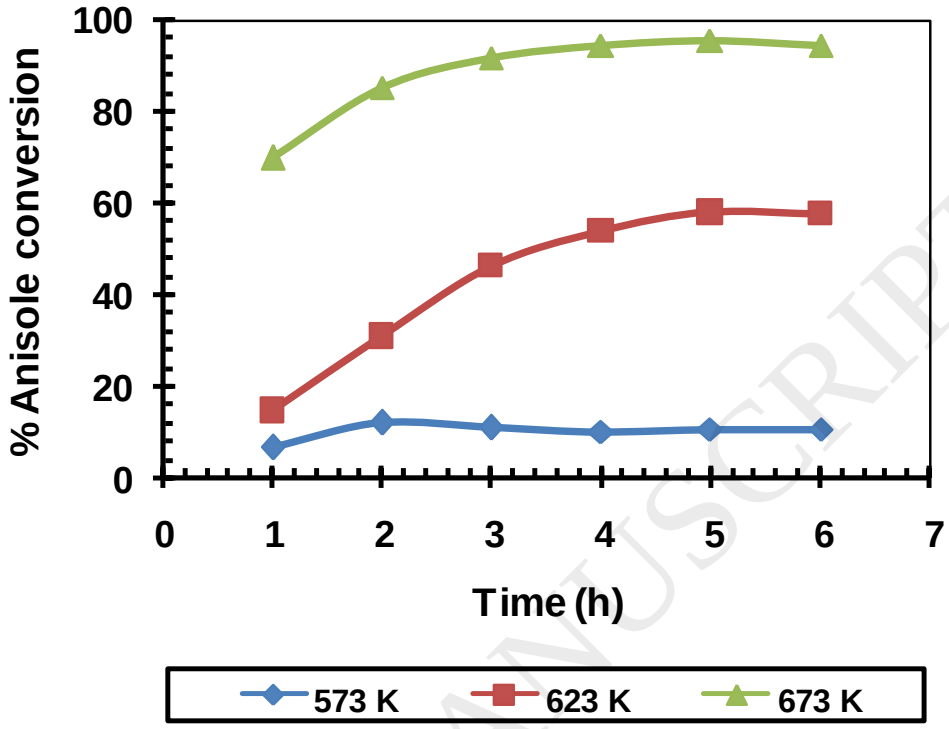

Figure 11(a). Anisole conversion at different temperatures. Reaction conditions - Anisole as reactant, catalyst – 2 g, WHSV – 1 h^{-1}, temperature – 573 - 673 K, N_2 flow – 30 mL/min

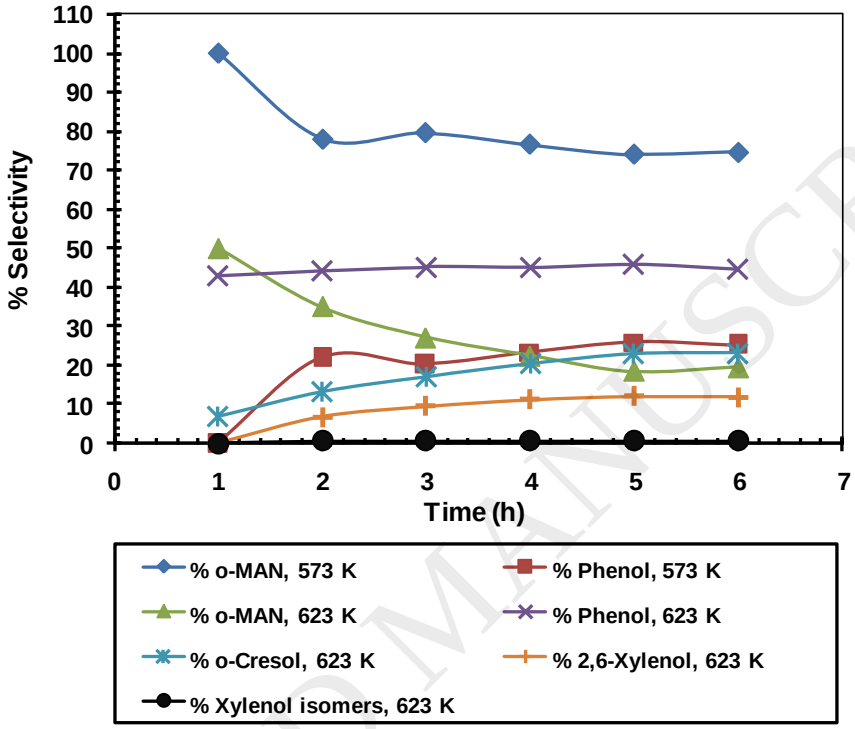

Figure 11(b). Product selectivity profile of anisole rearrangement at 573 K and 623 K. Reaction conditions - Anisole as reactant, catalyst – 2 g, WHSV – 1 h^{-1}, temperature – 573 - 673 K, N_2 flow – 30 mL/min

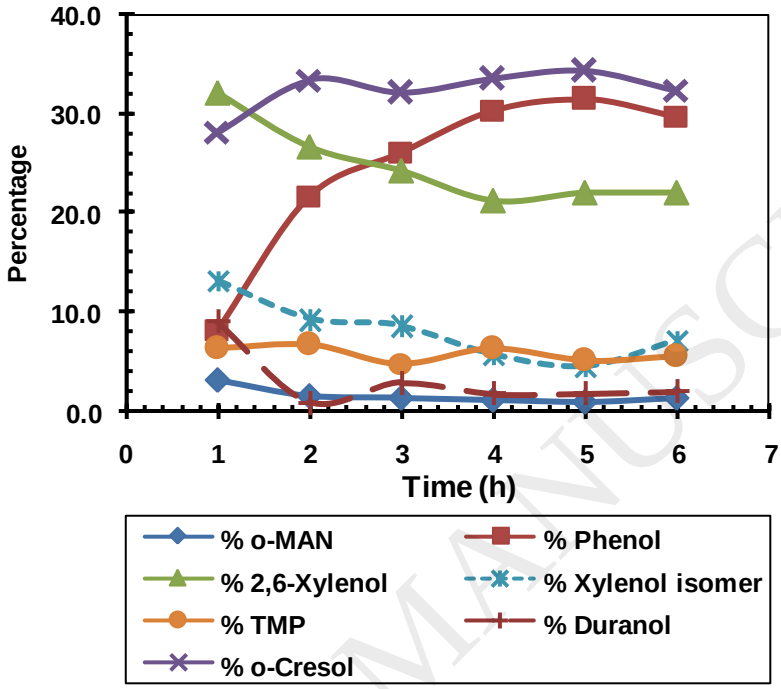

Figure 11(c). Products selectivity profile of rearrangement of anisole at 673K. Reaction conditions - Anisole as reactant, catalyst weight – 2 g, WHSV – 1 h^{-1}, temperature – 573 - 673 K, N_2 flow – 30 mL/min

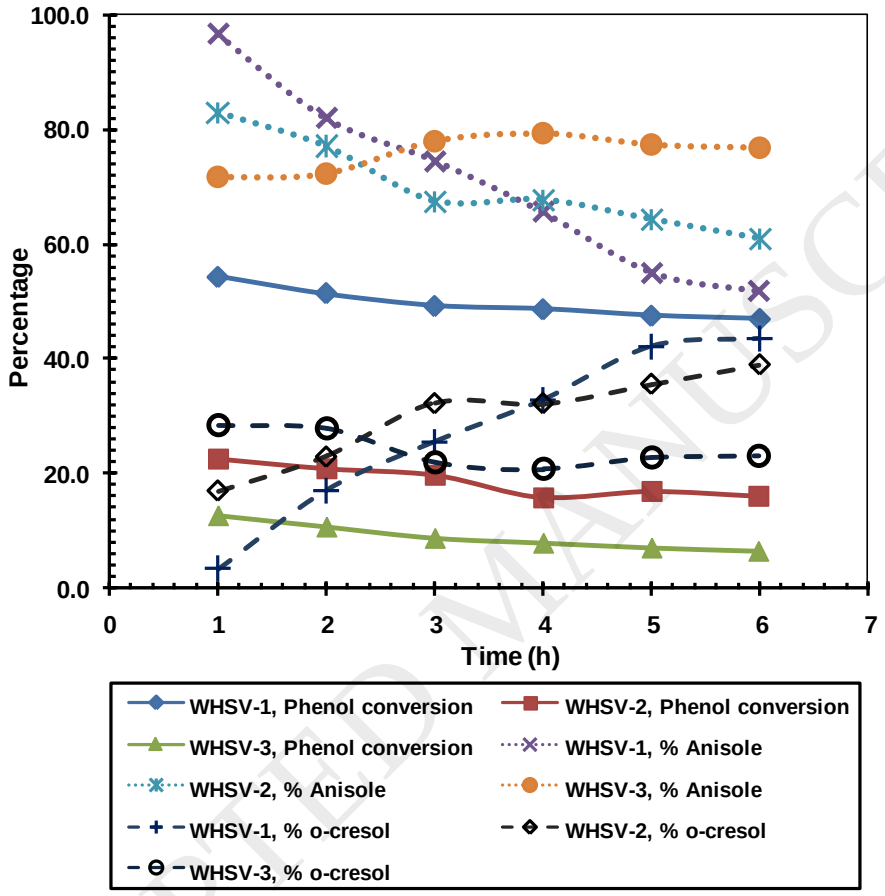

Figure 12. Effect of WHSV on methylation of phenol. Reaction conditions- Phenol: methanol (1:5) mole, catalyst– 2 g, WHSV – 1-3 h^{-1}, temperature – 623 K, N_2 flow – 30 mL/min

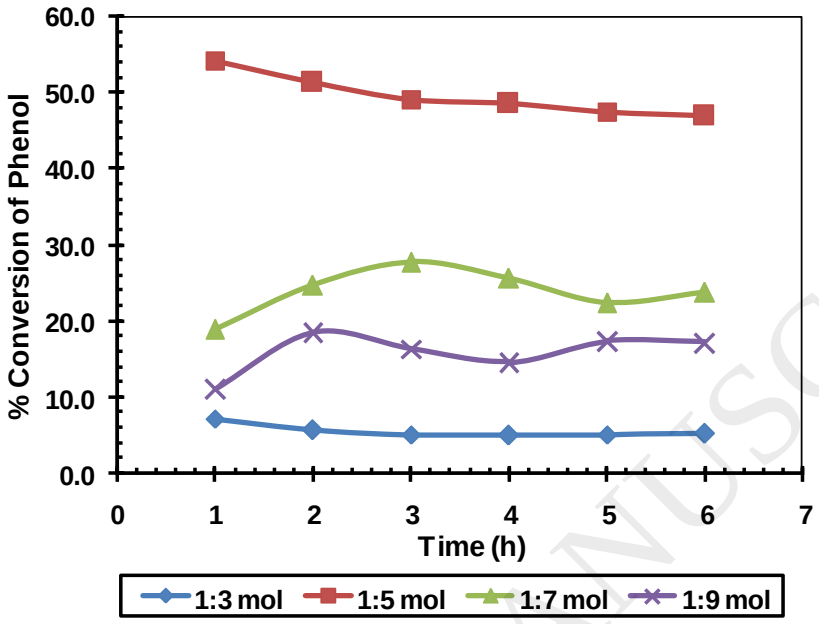

Figure 13(a). Effect of mole ratio on conversion of phenol. Reaction conditions- Phenol: methanol (1:3-1:9) mole, catalyst – 2 g, WHSV – 1 h^{-1}, temperature – 623 K, N_2 flow – 30 mL/min

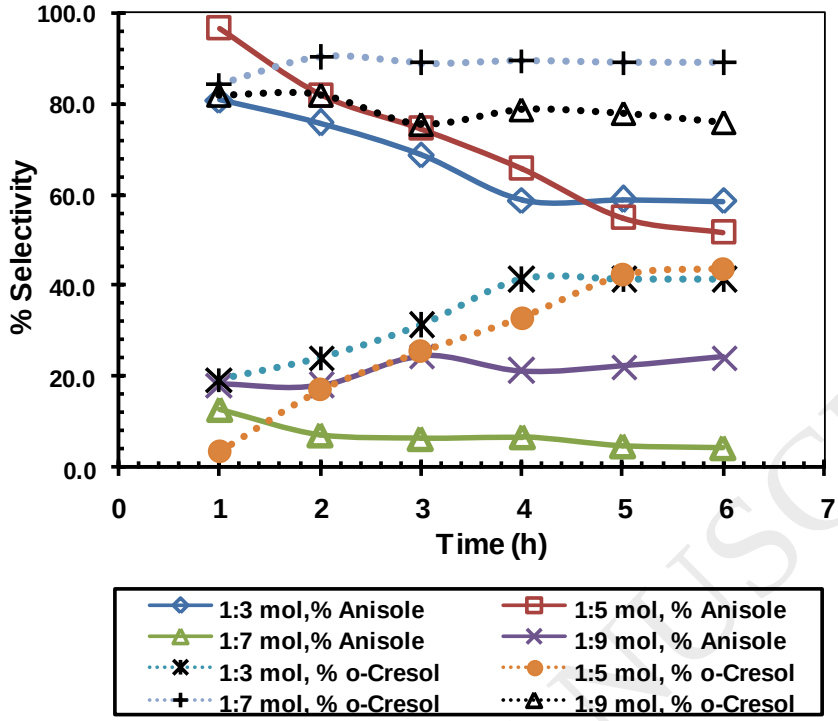

Figure 13(b). Effect of mole ratio on product selectivity. Reaction conditions- Phenol: methanol (1:3 - 1:9) mole, catalyst – 2 g, WHSV – 1 – 3 h^{-1}, temperature – 623 K, N_2 flow – 30 mL/min

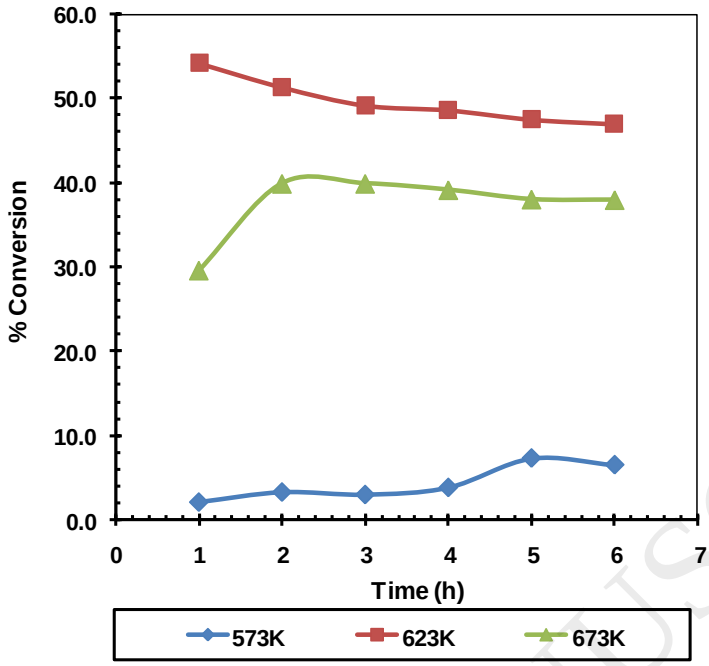

Figure 14(a). Effect of temperature on conversion of phenol. Reaction conditions- Phenol: methanol (1:5) mole, catalyst – 2 g, WHSV – $1h^{-1}$, temperature – 623- 673 K, N_2 flow – 30 mL/min

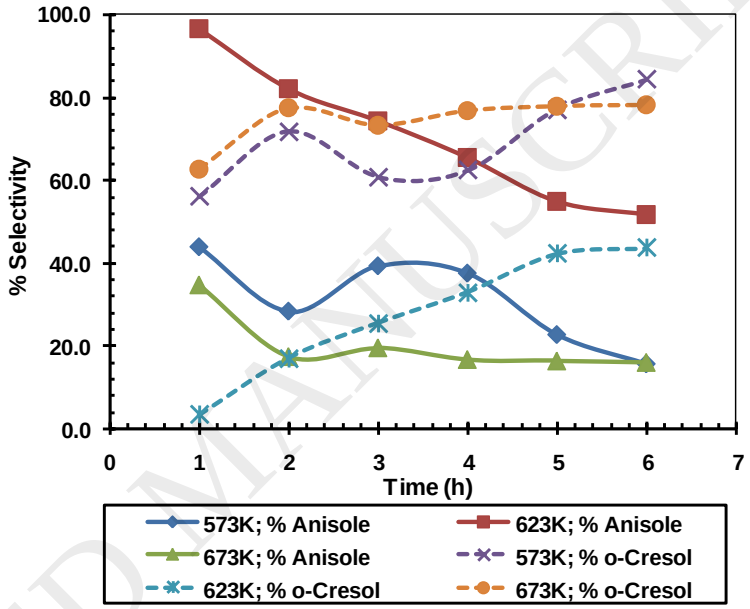

Figure 14(b). Effect of temperature on product selectivity. Reaction conditions- Phenol: methanol (1:5) mole, catalyst – 2 g, WHSV – 1 – 3 h^{-1}, temperature – 623- 673 K, N_2 flow – 30 mL/min

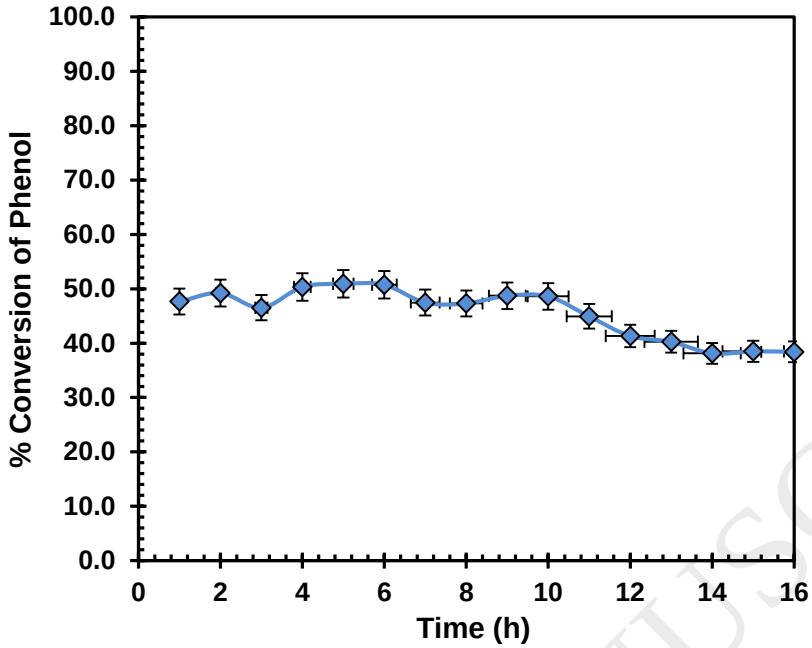

Figure 15(a). Time on stream study. Phenol conversion profile. Reaction conditions- Phenol: methanol (1:5) mole, catalyst – 2 g, WHSV – 1 h^{-1}, temperature – 623 K, N_2 flow – 30 mL/min

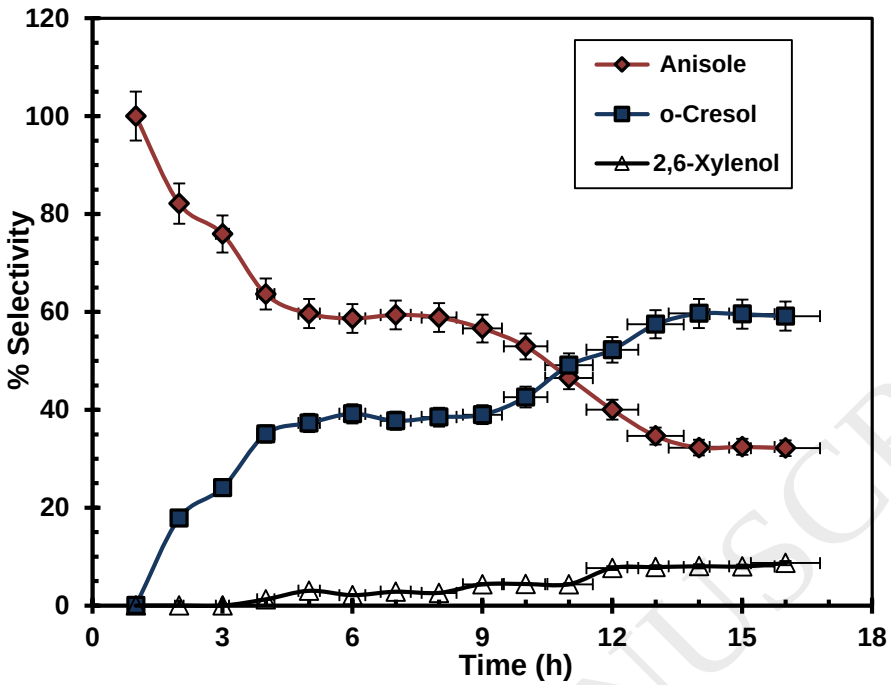

Figure 15(b). Time on stream study. Selectivity profile of products. Reaction conditions- Phenol: methanol (1:5) mole, catalyst – 2 g, WHSV – 1 h^{-1}, temperature – 623 K, N_2 flow – 30 mL/min

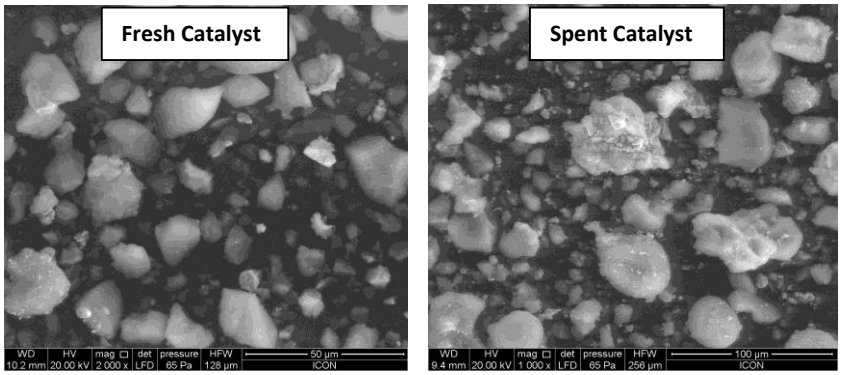

Figure 16. SEM images of fresh and spent 10%ZrO_2-30%WO_3-SiO_2 catalyst

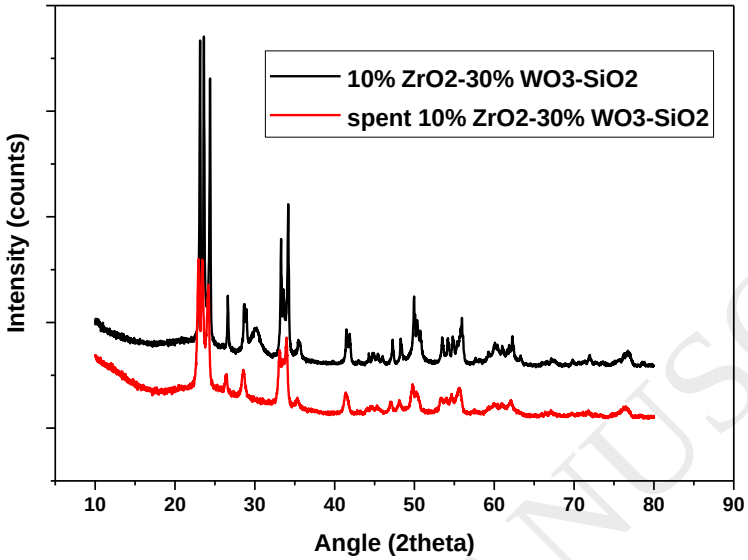

Figure 17. XRD comparison of fresh and spent 10%ZrO_2-30%WO_3-SiO_2

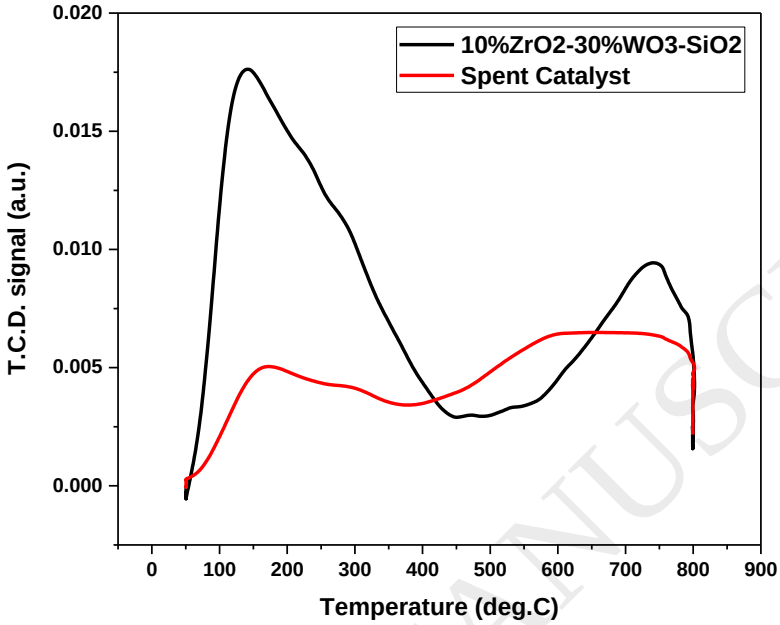

Figure 18. Ammonia TPD comparison of fresh and spent 10% ZrO_2-30%WO_3-SiO_2

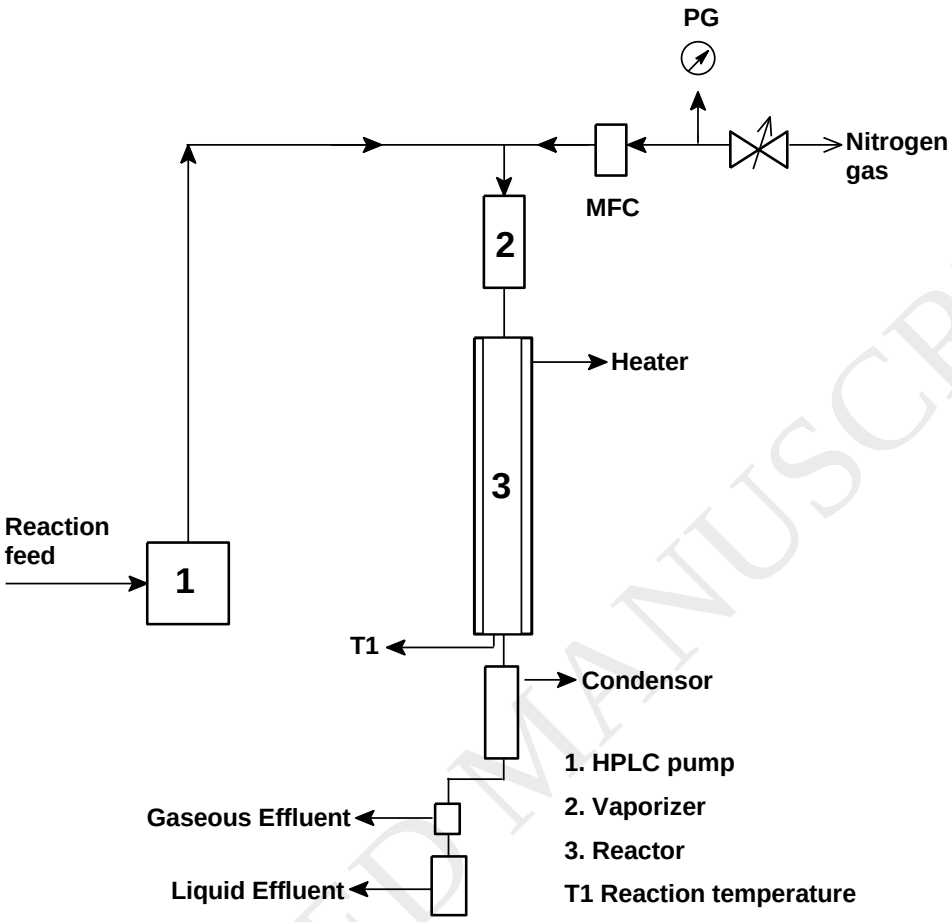

Scheme 1. Reactor Setup

5.

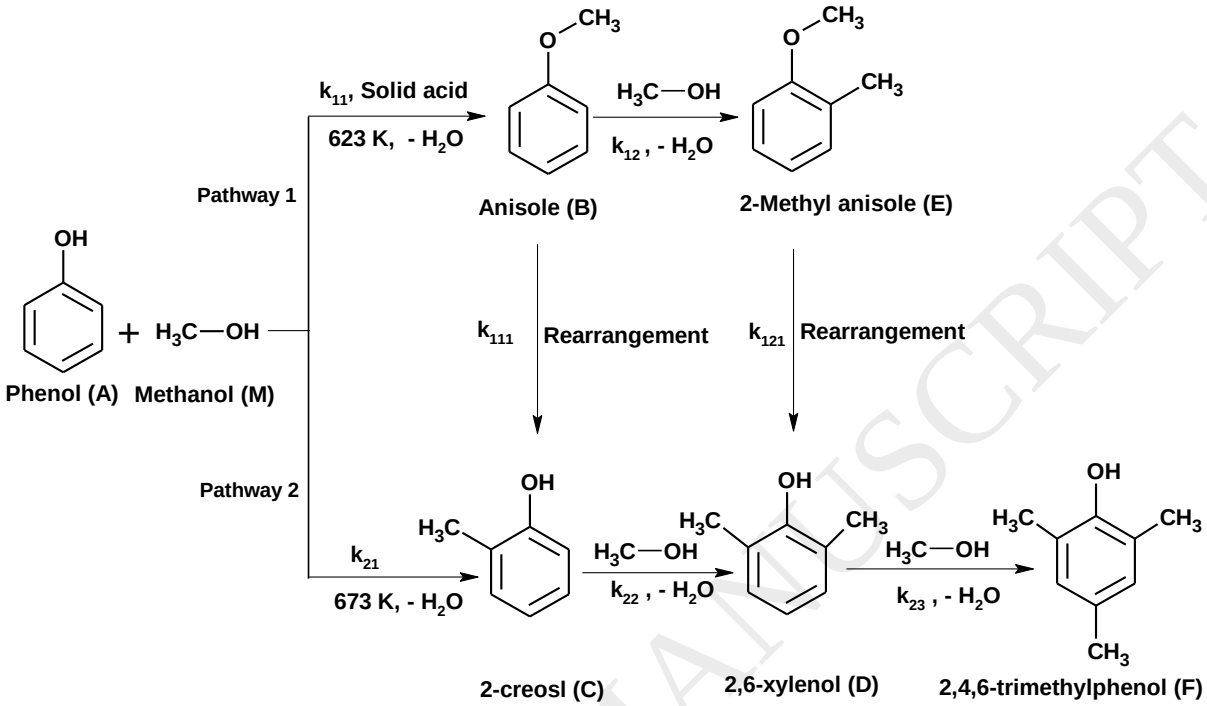

Scheme 2. Possible reaction pathways in methylation of phenol

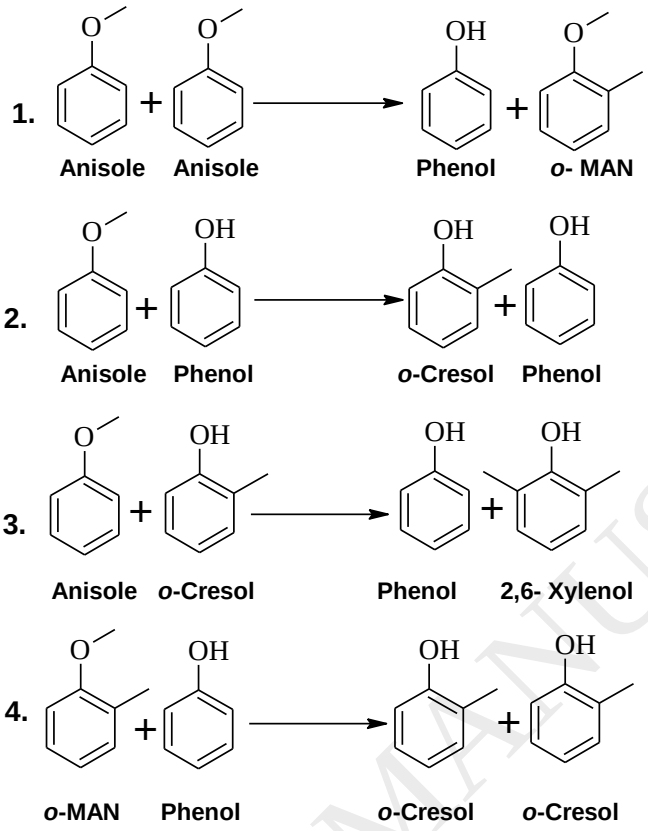

Scheme 3. Possible pathways in rearrangement of anisole

Tables

Table 1. Textural characteristics of *x*ZrO_2-*y*WO3-SiO_2 series catalysts

Catalyst	BET Surface area ($m^2\ g^{-1}$)	Avg. Pore Size[a] (nm)	Pore volume[b] ($cm^3\ g^{-1}$)
Aerosil-300	306.1	14.4	0.77
40Zr-Si	242.0	12.3	0.63
30Zr-10W-Si	182.8	15.7	0.72
20Zr-20W-Si	115.6	20.7	0.70
10Zr-30W-Si	97.6	29.8	0.79
40W-Si	100.9	17.4	0.46

[a]BJH desorption avg. pore size, [b]Single point adsorption total pore volume.

Table 2. Surface acidity of *x*ZrO_2-*y*WO3-SiO_2 series catalysts

Catalyst	**Desorption temp. (°C)**	**NH_3 desorbed (mmol/g)**	**Total NH_3 desorbed (mmol/g)**
40Zr-Si	138.9, 755.8	0.1406, 0.1476	0.288
30Zr-10W-Si	127.2, 677.0	0.1481, 0.2059	0.354
20Zr-20W-Si	128.5, 739.6	0.2057, 0.3129	0.518
10Zr-30W-Si	144.5, 740.3	0.3640,0.2712	0.635
40W-Si	124.5, 745.0	0.4648, 0.2223	0.687

Table 3. Elemental composition of *x*ZrO_2- *y*WO_3 - SiO_2 series catalysts

Catalyst sample	Expected Composition			Observed composition		
	% ZrO_2	**% WO_3**	**% SiO_2**	**% ZrO_2**	**% WO_3**	**% SiO_2**
40Z-Si	40	0	60	39.6	0	60.4
30Z -10W-Si	30	10	60	28.1	7.3	64.6
20Z-20W-Si	20	20	60	23.0	17.0	60.0
10Z-30W-Si	10	30	60	10.2	25.8	64.0
40W-Si	0	40	60	0	41.0	59.0

Table 4. Performance of $xZrO_2$-yWO_3 -SiO_2 series catalysts. Reaction conditions- Phenol: methanol (1:5) mole, catalyst – 2 g, WHSV – 1 h^{-1}, temperature – 623 K, N_2 flow – 30 mL/min, time – 6 h.

Catalyst	% Conversion[a]	% Anisole[b]	% Cresol[b]	% 2,6-Xylenol[b]	Others[c]
40Zr-Si	36	39.6	51.2	9.2	0
30Zr-10W-Si	42	34.9	53.4	11.7	0
20Zr-20W-Si	28	66.4	33.6	0	0
30W-10Zr-Si	47	51.8	43.6	4.6	0
40W-Si	37.5	56.1	42.2	1.7	0
20W-Zr	45.1	25.1	53.7	11.3	9.9
40W-Zr	51.4	38.4	47.2	10.1	4.3

[a] conversion calculated on the basis of GC results, [b] selectivity calculated on the basis of GC results
[c] selectivity of TMP and higher alkylated derivatives of phenol (based on GC results)

Table 5. Elemental composition of fresh & spent catalyst

Metal	Fresh catalyst (%)	Spent catalyst (%)
Si	24.8	22.8
Zr	5.7	3.5
W	19.4	17.2
O	50.1	44.3
C	-	12.3

Table 6. Characterization of fresh & spent catalyst

Tests	Fresh catalyst (%)	Spent catalyst (%)
Surface area (m^2/g)	97.6	94.8
Pore volume (cm^3/g)	0.79	0.71
Acidity (mmol/g)	0.6	0.27